Thermochimica Acta 501 (2010) 78–83

Contents lists available at ScienceDirect

Thermochimica Acta

journal homepage: www.elsevier.com/locate/tca

Thermal decomposition of allyl-imidazolium-based ionic liquid studied by TGA–MS analysis and DFT calculations

Yan Hao, Jing Peng*, Shaowen Hu*, Jiuqiang Li, Maolin Zhai

Beijing National Laboratory for Molecular Sciences (BNLMS), Department of Applied Chemistry, College of Chemistry and Molecular Engineering, Peking University, Beijing 100871, PR China

ARTICLE INFO

Article history:
Received 7 September 2009
Received in revised form
21 December 2009
Accepted 8 January 2010
Available online 18 January 2010

Keywords:
Ionic liquids
1-Allyl-3-methylimidazolium chloride
Thermal decomposition mechanisms and kinetics
Isothermal thermogravimetric analysis
Density functional theory calculations
TGA–MS

ABSTRACT

Thermal stability of ionic liquids (ILs) is of great significance for their applications in dissolving cellulose at elevated temperature. A novel ionic liquid, 1-allyl-3-methylimidazolium chloride ([Amim]Cl), was found to be a powerful solvent for cellulose. However, the study about long-term isothermal stability, thermal decomposition mechanism and decomposition products of [Amim]Cl are scarce. Herein, we studied the thermal stability and degradation mechanism of [Amim]Cl using isothermal thermogravimetric analysis (TGA) experiments and density functional theory (DFT) calculations. The weight loss of [Amim]Cl at 100 °C under air atmosphere within 15 days was only 1.9% and [Amim]Cl after long-term heating also had dissolving capability of cellulose, indicating that [Amim]Cl has high thermal stability and can be long-term used at the dissolving temperature of cellulose. Both TGA experiments and DFT calculations revealed [Amim]Cl decomposed along two channels and the main pyrolysis products of the proposed mechanisms were detected using thermogravimetric technique coupled with mass spectrometry (TGA–MS).

1. Introduction

Room temperature ionic liquids (RTILs), as new solvents, have been attracting immense attention for their high thermal stability and conductivity, low melting point, and wide electrochemical window [1–3]. Furthermore, the solvent properties of ionic liquids (ILs) can be well tuned through modifying the structure of cation or anion moieties. The negligible vapor pressure of ILs makes them a good alternative for the toxic and volatile conventional organic solvents [4,5].

As an abundant biopolymer on the earth, cellulose is renewable, biodegradable and applicable in fiber, paper, membrane, polymer, and paints industries [6]. However, because cellulose is usually composed of stiff molecular structures with various intermolecular and intramolecular hydrogen bonds, it is extremely difficult to dissolve in water and most common organic solvents [7]. The insolubility of cellulose has become a bottleneck for its application, and a number of substances have been developed as its solvents. To date, only a limited number of cellulose solvent systems have been found, such as LiCl–*N*,*N*-dimethylacetamide (DMAc) [8], *N*-methylmorpholine-*N*-oxide (NMMO) [9] and $LiClO_4{\cdot}3H_2O$. These solvents, however, have some limitations such as high cost, volatility, toxicity, instability, or may induce the degradation of cellulose [10]. In 2002, Swatloski et al. found that RTILs could dissolve cellulose efficiently [11]. This initiated an interest in the study of dissolution and functional modification of cellulose in RTILs. Recently, a novel ionic liquid, 1-allyl-3-methylimidazolium chloride ([Amim]Cl), was used to dissolve cellulose and carry out homogeneous reactions of cellulose. Compared to the saturated alkyl-imidazolium-based ILs, such as 1-butyl-3-methylimidazolium chloride ([Bmim]Cl), [Amim]Cl has superior solubility for cellulose under the identical dissolution condition [12]. Because cellulose cannot be dissolved in RTILs until heating at 60–110 °C, it is essential to study the thermal stability and decomposition mechanism of these RTILs at dissolving temperature of cellulose.

Up to date, onset decomposition temperature (T_{onset}) of several RTILs has been determined using scanning thermogravimetric analysis (TGA) method [12–14]. Kamavaram and Reddy investigated kinetics of thermal decomposition of [Bmim]Cl and 1-hexyl-3-methylimidazolium chloride ([Hmim]Cl) [15]. So far, only few attempts were made to investigate the long-term isothermal stability, the decomposition kinetics, thermal decomposition mechanism and decomposition products of [Amim]Cl, although this is rather significant for the application of dissolving cellulose.

In this work, the tentative and long-term thermal stability, thermal decomposition mechanisms and kinetics of [Amim]Cl were investigated and compared in detail using TGA experiments and density functional theory (DFT) calculations, which is a useful tool

* Corresponding authors. Tel.: +86 10 62757193; fax: +86 10 62757193.
E-mail addresses: jpeng@pku.edu.cn (J. Peng), swhu@pku.edu.cn (S. Hu).

0040-6031/$ – see front matter © 2010 Elsevier B.V. All rights reserved.
doi:10.1016/j.tca.2010.01.013

to predict the thermal stability of RTILs. The main degradation products of [Amim]Cl were also validated by thermogravimetric technique coupled with mass spectrometry (TGA–MS) experiments. The reported data suggested that TGA–MS had significant potential for the identification of decomposition products of RTILs. All these issues were particularly important for the design and selection of a suitable ionic liquid for dissolving cellulose.

2. Experimental

2.1. Materials

[Amim]Cl (>99%) was provided by Institute of Chemistry, Chinese Academy of Sciences (Beijing, China). [Bmim]Cl (>99%) was purchased from Lanzhou Institute of Chemical Physics (Lanzhou, China). The water contents in the [Amim]Cl and [Bmim]Cl samples, measured using Karl-Fischer titration, were less than 0.3% and 0.9%, respectively.

2.2. Analytical methods

SDT Q600 (TA Instrument, USA) with alumina crucibles was used to perform TGA experiments. A constant heating rate of 10 °C min^{-1} and gas purging at a flow rate of 100 mL min^{-1} was used for all experiments. The amount of samples used for TGA was ca. 8 mg. The scanning TGA experiments were performed in nitrogen and air atmospheres, respectively. The resulting T_{onset} was determined from the step tangent. Long-term thermal stability of ILs was investigated using isothermal TGA under nitrogen atmosphere at each constant temperature in the temperature range of 150–190 °C for 800 min. Whereas, the gravimetrical experiment of [Amim]Cl was carried out in the oven at 100 °C under air atmosphere using P_2O_5 as desiccant.

Thermogravimetric technique coupled with mass spectrometry (TGA–MS) using STA 449C/QMS 403C (NETZSCH, Germany) instrument was employed to analyze the thermal decomposition products in situ. The TGA–MS experiments were performed from ambient temperature to 450 °C with a heating rate of 10 °C min^{-1} in argon gas purging at a flow rate of 100 mL min^{-1}. The signal intensity of gaseous products during the heating was measured in situ using mass spectrum.

The geometry structures of all stationary points on the potential energy surfaces were fully optimized using the density functional with general gradient approximation (GGA) methods incorporated with all-electron TZ2P basis set. For each GGA optimized structure, analytical frequency calculation using the same GGA method was performed to characterize the structure as either a minimum or a transition state. Then single point calculation using hybrid density functional B3LYP incorporated with all-electron TZ2P basis set was performed. Because the B3LYP density functional has been widely used in computational works for many molecular systems, and was suggested as a suitable tool to study the thermal dissociation mechanism of some ILs [16], we chose this functional to get the final energies with GGA optimized structures. ADF2007 program package [17–19] was employed for all the calculations.

3. Results and discussion

3.1. T_{onset} and long-term thermal degradation kinetics of [Amim]Cl

According to the scanning TGA experiments, the T_{onset} of [Amim]Cl was 249 °C under nitrogen atmosphere with a constant heating rate of 10 °C min^{-1}. This result was lower than the result previously reported (273 °C) [12], due to the differences of sample weight, the water contents of [Amim]Cl samples and heating rate [20,21]. Changing atmosphere from nitrogen to air only lowers the T_{onset} by 1 °C for [Amim]Cl, due to the very low solubility of oxygen in the imidazolium-based ILs [22]. However, T_{onset} is obtained by quick heating, which often overrates the thermal stability of RTILs due to the nature of scanning TGA. To evaluate the thermal stability of [Amim]Cl precisely, which is important for industrial applications, long-term investigation using isothermal TGA at each temperature interval is necessary.

Long-term thermal stability and thermal degradation kinetics of [Amim]Cl were studied in the temperature range of 150–190 °C. At 190 °C, the sample weight loses up to 98.7% after heating for 800 min under flowing nitrogen atmosphere. Apparently, when heating for longer time, the decomposition temperature of [Amim]Cl is considerably lower than T_{onset} (249 °C) determined using scanning TGA method.

Fig. 1 shows a linear weight decrease of [Amim]Cl sample versus time in the temperature range of 150–180 °C, implying that the thermal decomposition kinetics obeys a pseudo-zero-order rate law [15,23]. The rate expression at a constant temperature is:

$$\frac{d\alpha}{dt} = k \tag{1}$$

or

$$\alpha = kt + C \tag{2}$$

where k is the rate constant, C is an integral constant, and α is the degree of conversion defined as the ratio of sample weight (W) lost:

$$\alpha = \frac{W_i - W_t}{W_i} \tag{3}$$

For the linear part of the α/t curves shown in Fig. 1, the rate constant (k) at certain temperature can be determined from the slope of the corresponding curve.

In order to evaluate the activation energy (E_a) of the thermal decomposition according to the Arrhenius law:

$$k = A \ \exp\left(\frac{-E_a}{RT}\right) \tag{4}$$

We plotted the ln k versus $1/T$ curve as shown in Fig. 2. From the intercept and slope of the curve, the pre-exponential coefficient A and E_a were calculated as 3.0×10^{13} and 125 kJ mol^{-1}, respectively. All values were measured in triplicate with uncertainty within 5%.

To fully evaluate the long-term thermal stability of [Amim]Cl at the operating temperature of dissolving cellulose, we also measured the weight loss of [Amim]Cl at 100 °C under air atmosphere using gravimetrical method. As shown in Fig. 3, the weight loss of sample was only 1.9% after heating at 100 °C for 15 days. And

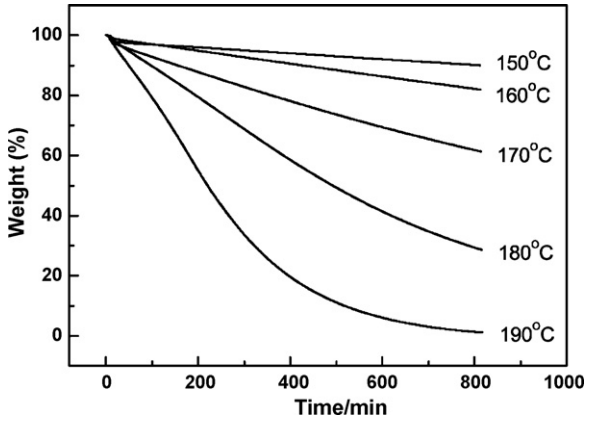

Fig. 1. Isothermal decomposition of [Amim]Cl in the temperature range of 150–190 °C under flowing nitrogen atmosphere.

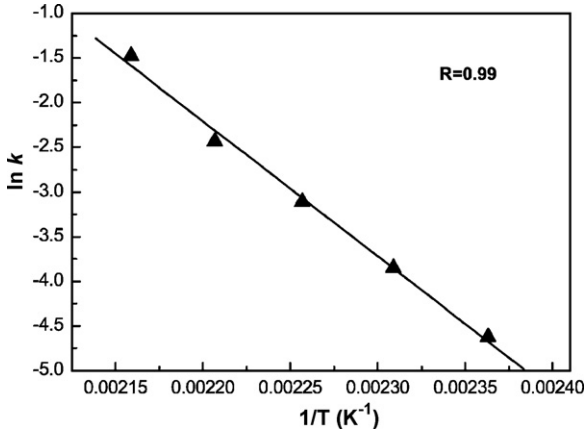

Fig. 2. Arrhenius plot for the decomposition of [Amim]Cl in the temperature range of 150–190 °C under flowing nitrogen atmosphere.

[Amim]Cl after long-term heating also had dissolving capability of cellulose, indicating that [Amim]Cl has high thermal stability and can be long-term used as cellulose solvent at such temperature.

For comparison, long-term thermal stability and thermal degradation kinetics of [Bmim]Cl were also investigated under the identical experimental conditions. Using the isothermal TGA curves at 150 °C, the actual rates of weight loss were calculated for the two ILs. The results indicated that the decomposition of [Bmim]Cl was slower than that of [Amim]Cl, another evidence of which was the colour changes of both ILs during heating process [24]. Under identical experiment condition, the colour changes of [Amim]Cl were more obvious than that of [Bmim]Cl after heating at 100 °C for 15 days. Moreover, the pre-exponential coefficient A and activation energy E_a of [Bmim]Cl were calculated as 2.8×10^{13} and 129 kJ mol^{-1}. The E_a of [Bmim]Cl is slightly higher than that of [Amim]Cl.

3.2. Mechanism of thermal decompositions

Quantum chemical calculations are a useful tool to predict the thermal decomposition mechanisms and kinetics of ILs. Fig. 4(a) shows the structure of species involved in [Amim]Cl pyrolysis along a two-channel mechanism. [Amim]Cl has three conformers A1, A2, A3, owing to the free C–N or C–C single bond rotation. The anion Cl forms a bond with the acidic H atom connected to C2. The electron attracting effect of the double bond makes Cl tilt slightly towards the allyl group. In channel one [Amim]Cl dissociate via transition states ATS1, ATS2, and ATS3, forming products A4, A5, A6, which are three conformers of allyl imidazole (AIM) weakly bonded with methyl chloride. The activation energy for this channel, evaluated as the energy difference between the transition states and the most stable conformer of the reactant [Amim]Cl, is in the range of 123–124 kJ mol^{-1}. In channel two [Amim]Cl dissociates via transition states ATS4 or ATS5, resulting in complex A7, in which allyl chloride hydrogen bonds to methylimidazole (MIM). Relative to A1, the activation energy is 120–122 kJ mol^{-1}. Compared with channel one, it can be seen that the allyl group is a little easier to dissociate than methyl group. In both channel, the dissociated products are thermodynamically more stable than their ILs forms. For A7, the extra stability may result from the hydrogen bond formed between allyl chloride and MIM.

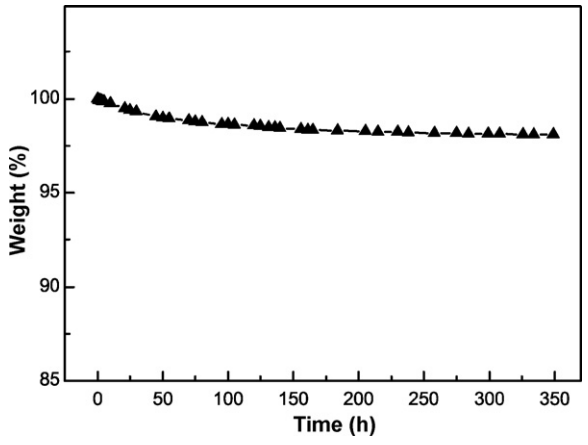

Fig. 3. The weight changes of [Amim]Cl at 100 °C under air atmosphere within 15 days.

There are several conformers of [Bmim]Cl owing to the flexibility of its butyl side chain. Only two most stable conformers are shown in Fig. 4(b). Unlike the conformers of [Amim]Cl, the anion Cl of [Bmim]Cl tilts away from the butyl side chain. [Bmim]Cl can also dissociate along two channels. In channel one [Bmim]Cl dissociates into 1-butylimidazole (BIM) and methyl chloride. The transition state with the lowest relative energy is BTS1. B3 is the product in which BIM weakly associates to methyl chloride. The activation energy of this channel is 122 kJ mol^{-1}, similar with that of [Amim]Cl dissociating along channel one, indicating that the side chain connected to N1 has little effect on the cleavage of the methyl group connected to N3. In channel two [Bmim]Cl dissociates via transition state BTS2, resulting in B4, a weakly associated complex of MIM and butyl chloride. The activation energy of this channel is 134 kJ mol^{-1}, considerably larger than that of channel one. The longer alkyl side chain has a kinetic stable effect on the IL. Similar to [Amim]Cl, in both channels, the dissociated products are thermodynamically more stable than their ILs forms.

Therefore, the thermal decompositions of the two ILs are mainly kinetic controlled process. Because of the higher average activation energy of decomposition [Bmim]Cl appears tentatively more stable and decomposes slower than [Amim]Cl.

Although the calculated activation energies are quite close to the experimental data, it should be mentioned that because the calculations simplified the ionic liquids as single molecules using an ideal gas model at absolute zero degree, only relative energies between the species are significant.

3.3. Thermal degradation products of [Amim]Cl

Thermal degradation products of [Amim]Cl were investigated using TGA–MS to verify the decomposition mechanisms proposed in the former paragraph.

Fig. 5 shows the MS signal intensity of various gaseous decomposition products of [Amim]Cl (a) and [Bmim]Cl (b) as a function of temperature. It can be seen that the ion current enhances rapidly at 200–350 °C, indicating that the decompositions mainly proceed at this temperature interval.

The mass to charge ratios (m/z) (amu) detected as products of [Amim]Cl pyrolysis were assigned to methyl chloride (m/z: 50), allyl chloride (m/z: 76), MIM (m/z: 82), AIM (m/z: 108) and some fragmented charged species, such as CH_3^+ (m/z: 15) and C_2H_2 (m/z: 26). Among the mass to charge ratios detected, the signal intensity of CH_3^+ was the strongest, because the CH_3^+ group was the main fragmented charged species produced by MIM and methyl chloride [24]. The results of TGA–MS indicated that pyrolysis of [Amim]Cl proceeded along two pathways, one leading to formation of allyl chloride and MIM, the other leading to formation of methyl chloride and AIM (Scheme 1), which was consistent with the results proposed using DFT methods in Fig. 5(a). Furthermore [Amim]Cl decomposed through a C–N bond cleavage

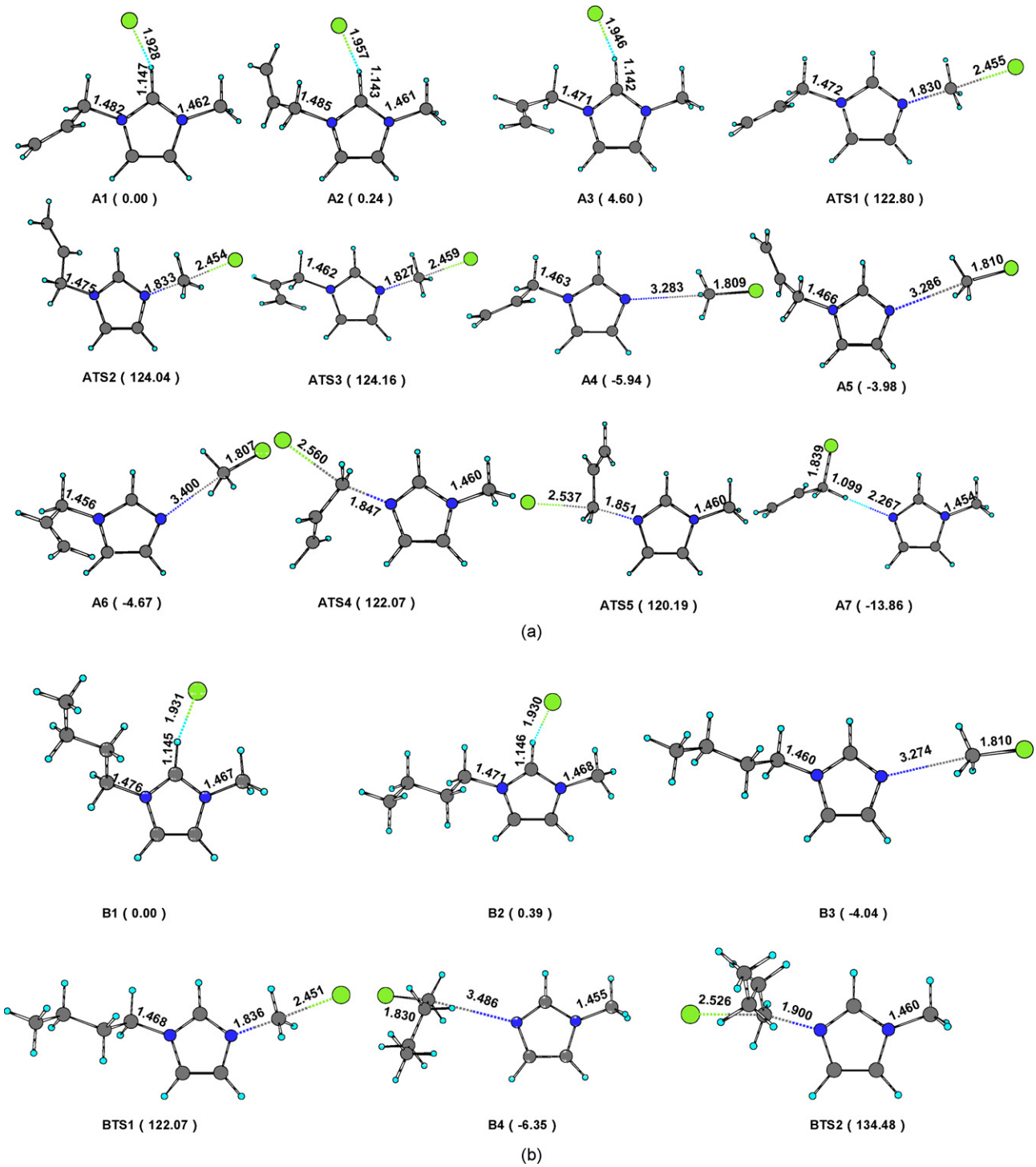

Fig. 4. Geometry structure of species involved in decomposition of [Amim]Cl (a) and [Bmim]Cl (b); bond lengths are in Å; relative energies (in parenthesis) are in kJ mol^{-1}.

at an alkyl group by the nucleophilic attack of chloride ion. During the heating process [Amim]Cl decomposed into allyl chloride (m/z: 76) and MIM (m/z: 82) at low temperature, followed by the further decomposition of allyl chloride simultaneously to form methyl chloride (m/z: 50) and C_2H_2 (m/z: 26). With the increase of temperature to around 350 °C, an obvious fluctuation of ion current was observed in TGA–MS curve for decomposition of [Amim]Cl. As shown in Fig. 5(a), the fluctuation was assigned to the other decomposition route of [Amim]Cl. In this case [Amim]Cl decomposed into methyl chloride (m/z: 50) and AIM (m/z: 108), accompanied by the further decomposition of AIM simultaneously, leading to the formation of MIM (m/z: 82) and C_2H_2 (m/z: 26).

For comparison, thermal degradation products of [Bmim]Cl were also investigated using TGA–MS. The mass to charge ratios (m/z) (amu) detected as products of [Bmim]Cl (m/z: 174) pyrolysis were assigned to CH_3^+ (m/z: 15), ethylene (m/z: 28), propylene (m/z: 42), methyl chloride (m/z: 50), ethyl chloride (m/z: 64), MIM (m/z: 82) and ethylimidazole (m/z: 96). Although the TGA–MS results are more complicated, it can still be inferred that the pyrolysis of [Bmim]Cl proceeds along two pathways, one leading to the formation of butyl chloride (m/z: 92) and MIM, the other lead-

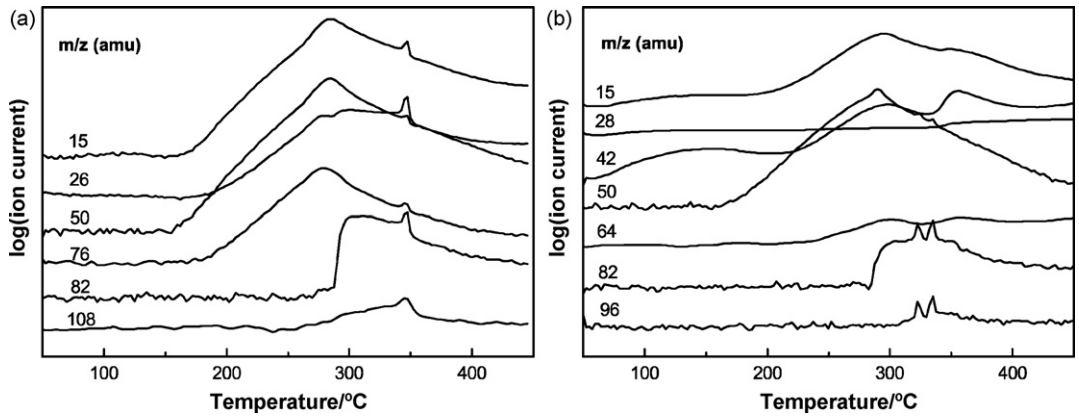

Fig. 5. TGA–MS curve for decomposition of [Amim]Cl (a) and [Bmim]Cl (b) at a heating rate of 10 °C min^{-1} under argon atmosphere.

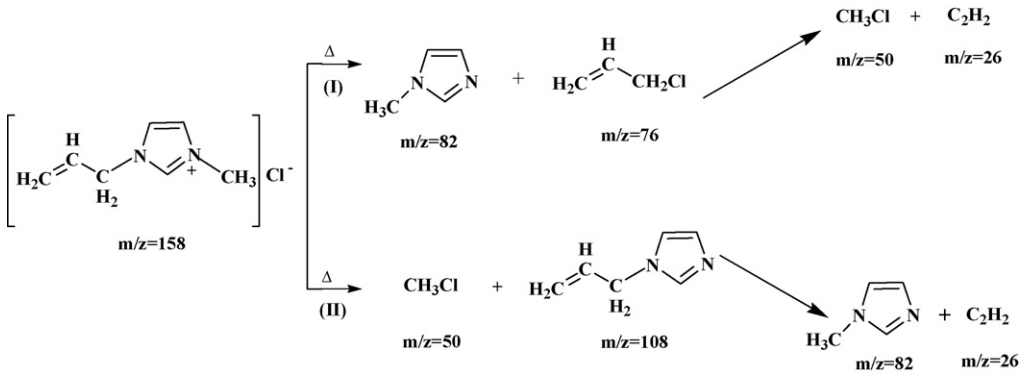

Scheme 1. Thermal degradation pathway of [Amim]Cl.

ing to the formation of methyl chloride and BIM (*m*/*z*: 124) forms. Further decomposition of butyl chloride and BIM may be the reason that the two species were not detected directly. Among the detected fragment species, ethyl chloride and ethylene should be the dissociation products of butyl chloride; MIM, propylene, ethylimidazole and ethylene should be the dissociation products of BIM (Scheme 2).

Therefore, the TGA–MS results of [Amim]Cl and [Bmim]Cl agree well with the mechanism predicted via theoretical calculations.

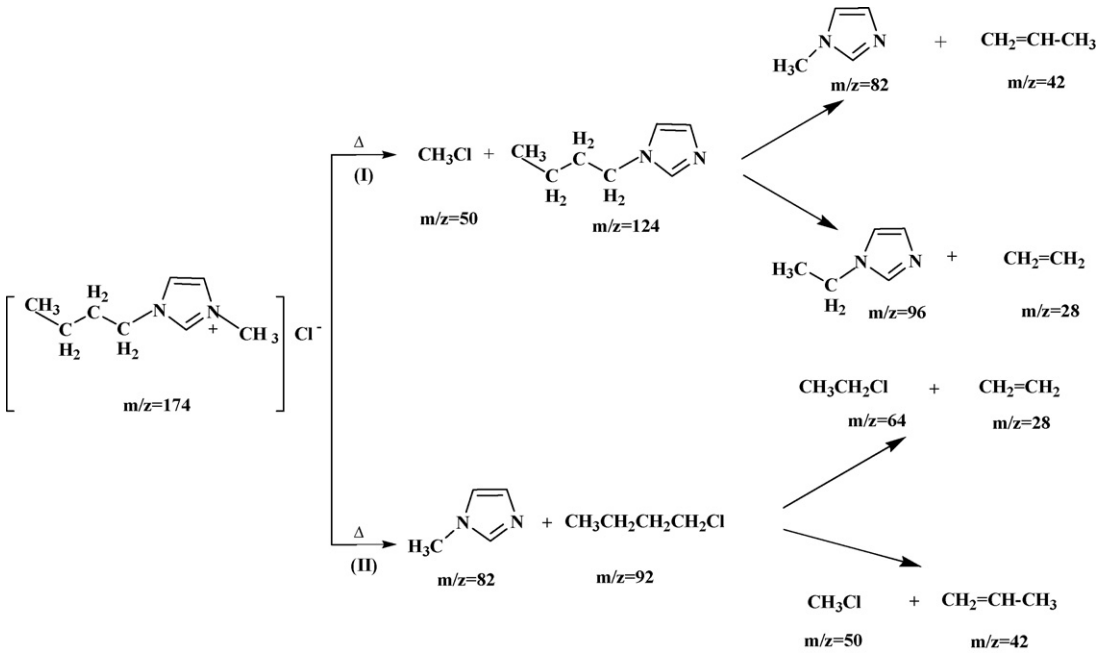

Scheme 2. Thermal degradation pathway of [Bmim]Cl.

4. Conclusions

[Amim]Cl has high thermal stability and can be long-term used at the operating temperature of dissolving cellulose. During the heating process, the allyl side chain of [Amim]Cl appears to associate with anion Cl and dissociate from imidazole ring with equal probability as the methyl group does, and the main pyrolysis products of the proposed mechanisms were detected using TGA–MS. Compared with [Amim]Cl, [Bmim]Cl is tentatively more stable and decomposes slower.

Acknowledgement

This work was financially supported by National Key Technology R&D Program (2006BAC02A10).

References

[1] J. Dupont, R.F. de Souza, P.A.Z. Suarez, Chem. Rev. 102 (2002) 3667–3691.
[2] C.E. Song, Chem. Commun. (2004) 1033–1043.
[3] R. Bini, C. Chiappe, C. Duce, A. Micheli, R. Solaro, A. Starita, M.R. Tine, Green Chem. 10 (2008) 314–317.
[4] T. Welton, Chem. Rev. 99 (1999) 2071–2083.
[5] J.G. Huddleston, A.E. Visser, W.M. Reichert, H.D. Willauer, G.A. Broker, R.D. Rogers, Green Chem. 3 (2001) 156–164.
[6] J. Schurz, Prog. Polym. Sci. 24 (1999) 481–483.
[7] L. Feng, Z.I. Chen, J. Mol. Liq. 142 (2008) 1–5.
[8] M. Terbojevich, A. Cosani, G. Conio, A. Ciferri, E. Bianchi, Macromolecules 18 (1985) 640–646.
[9] T. Heinze, T. Liebert, Prog. Polym. Sci. 26 (2001) 1689–1762.
[10] J. Wu, J. Zhang, H. Zhang, J.S. He, Q. Ren, M. Guo, Biomacromolecules 5 (2004) 266–268.
[11] R.P. Swatloski, S.K. Spear, J.D. Holbrey, R.D. Rogers, J. Am. Chem. Soc. 124 (2002) 4974–4975.
[12] H. Zhang, J. Wu, J. Zhang, J.S. He, Macromolecules 38 (2005) 8272–8277.
[13] P. Bonhote, A.P. Dias, M. Armand, N. Papageorgiou, K. Kalyanasundaram, M. Gratzel, Inorg. Chem. 37 (1998) 166–1166.
[14] H.L. Ngo, K. LeCompte, L. Hargens, A.B. McEwen, Thermochim. Acta 357 (2000) 97–102.
[15] V. Kamavaram, R.G. Reddy, Int. J. Therm. Sci. 47 (2008) 773–777.
[16] M.C. Kroon, W. Buijs, C.J. Peters, G.J. Witkamp, Thermochim. Acta 465 (2007) 40–47.
[17] G.T. Velde, F.M. Bickelhaupt, E.J. Baerends, C.F. Guerra, S.J.A. Van Gisbergen, J.G. Snijders, T. Ziegler, J. Comput. Chem. 22 (2001) 931–967.
[18] C.F. Guerra, J.G. Snijders, G. te Velde, E.J. Baerends, Theor. Chem. Acc. 99 (1998) 391–403.
[19] ADF2007.01, SCM, Theoretical Chemistry, Vrije Universiteit, Amsterdam, The Netherlands, http://www.scm.com.
[20] M. Kosmulski, J. Gustafsson, J.B. Rosenholm, Thermochim. Acta 412 (2004) 47–53.
[21] M.E. Van Valkenburg, R.L. Vaughn, M. Williams, J.S. Wilkes, Thermochim. Acta 425 (2005) 181–188.
[22] J.L. Anthony, J.L. Anderson, E.J. Maginn, J.F. Brennecke, J. Phys. Chem. B 109 (2005) 6366–6374.
[23] K.J. Baranyai, G.B. Deacon, D.R. MacFarlane, J.M. Pringle, J.L. Scott, Aust. J. Chem. 57 (2004) 145–147.
[24] R.E. Del Sesto, T.M. McCleskey, C. Macomber, K.C. Ott, A.T. Koppisch, G.A. Baker, A.K. Burrell, Thermochim. Acta 491 (2009) 118–120.